

Constitutive property behavior of an ultra-high-performance concrete with and without steel fibers

E.M. Williams*, S.S. Graham, S.A. Akers, P.A. Reed and T.S. Rushing

U.S. Army Engineer Research and Development Center, Geotechnical and Structures Laboratory, Vicksburg, MS, USA

(Received July 29, 2009, Accepted August 7, 2009)

Abstract. A laboratory investigation was conducted to characterize the constitutive property behavior of Cor-Tuf, an ultra-high-performance composite concrete. Mechanical property tests (hydrostatic compression, unconfined compression (UC), triaxial compression (TXC), unconfined direct pull (DP), uniaxial strain, and uniaxial-strain-load/constant-volumetric-strain tests) were performed on specimens prepared from concrete mixtures with and without steel fibers. From the UC and TXC test results, compression failure surfaces were developed for both sets of specimens. Both failure surfaces exhibited a continuous increase in maximum principal stress difference with increasing confining stress. The DP tests results determined the unconfined tensile strengths of the two mixtures. The tensile strength of each mixture was less than the generally assumed tensile strength for conventional strength concrete, which is 10 percent of the unconfined compressive strength. Both concretes behaved similarly, but Cor-Tuf with steel fibers exhibited slightly greater strength with increased confining pressure, and Cor-Tuf without steel fibers displayed slightly greater compressibility.

Keywords: ultra-high-performance concrete; steel fibers; mechanical response.

1. Introduction

Cor-Tuf is the name given to a family of ultra-high-performance concretes (UHPCs) developed at the U.S. Army Engineer Research and Development Center (ERDC). UHPCs are distinguished from other concretes by their high compressive strengths (up to 200 MPa). The Cor-Tuf composition was designed to develop ultra-high compressive strength while maintaining workability and production economy. Most UHPCs, such as Cor-Tuf, can be broadly characterized as reactive powder concretes because the concretes are composed of fine aggregate and pozzolanic powders but do not include the coarse aggregate generally found in conventional concrete mixtures. Table 1 shows the mixture composition for Cor-Tuf.

Batches of Cor-Tuf produced for this study were designated Cor-Tuf1, which contained Bekaert Corporation's Dramix® ZP305 steel fibers, and Cor-Tuf2, which had no steel fibers. In general, the inclusion of steel fibers in a concrete mixture increases the ductility of the material; therefore, mechanical property tests were conducted on specimens prepared from each batch of Cor-Tuf. The test specimens were cut and the ends ground flat and parallel to each other and perpendicular to the sides of the core in accordance with procedures for preparing rock core in American Society for

* Corresponding author, E-mail: erin.m.williams@usace.army.mil

Table 1 Cor-Tuf mixture composition

Material	Product	Proportion by Weight
Cement	Lafarge, Class H, Joppa, MO	1.00
Sand	US Silica, F55, Ottawa, IL	0.967
Silica flour	US Silica, Sil-co-Sil 75, Berkeley Springs, WV	0.277
Silica fume	Elkem, ES 900 W	0.389
Superplasticizer	W.R. Grace, ADVA 170	0.0171
Water (tap)	Vicksburg, MS municipal water	0.208
Steel fibers ¹	Bekaert, Dramix® ZP305	0.310

¹Steel fibers used in Cor-Tuf1 material only.

Testing and Materials (ASTM) D 4543 (ASTM 2009). Each prepared test specimen had a nominal height of 110 mm and a diameter of 50 mm. Twenty-three quasi-static mechanical property tests (hydrostatic compression (HC), unconfined compression (UC), triaxial compression (TXC), unconfined direct pull (DP), uniaxial strain (UX), and uniaxial-strain-load/constant-volumetric-strain (UX/CV) tests) were conducted on specimens from each batch of Cor-Tuf.

2. Mechanical property tests

All of the mechanical property tests were conducted with axial strain rates on the order of 10^{-4} to 10^{-5} /sec and times to peak load on the order of 5 to 30 min. Undrained isotropic compressibility data were obtained from HC tests and during the hydrostatic loading phases of the TXC tests. Shear and failure data were obtained from UC tests, unconsolidated-undrained TXC tests, and DP tests. The terms *unconsolidated* and *undrained* signify that no pore fluid (liquid or gas) was allowed to escape or drain from the membrane-enclosed specimens. One-dimensional compressibility data were obtained from undrained UX tests via lateral stress measurements. The strain path tests were initially loaded under uniaxial strain boundary conditions to a prescribed level of axial stress. At the end of the UX loading, a constant axial-to-radial-strain ratio (ARSR) of -2.0 was applied. The ARSR=-2.0 path is a constant-volumetric-strain path; these tests will be referred to as UX/CV tests.

2.1. Test devices and instrumentation

Three sets of test devices were used in this test program. The axial load for all UC tests was provided by a 3.3-MN loader, which was manually controlled. The UC tests required only a specimen top and base cap, load cell, and vertical and radial deformeters.

The DP tests used end caps that were attached to the unconfined specimens with Sikadur® Crack Fix structural epoxy. A manual hydraulic pump pressurized the underside of a flange that was attached to both the piston and the test specimen. The piston's retraction produced the tensile load on the specimen, and the load cell recorded the measurements of the applied axial load on the specimen.

All remaining tests were conducted in a 600-MPa-capacity pressure vessel (Fig. 1), with the axial load provided by an 8.9-MN loader. With this loader and its associated hydraulic pump, a servo-controlled data acquisition system regulated the application of load, pressure, and axial displacement.

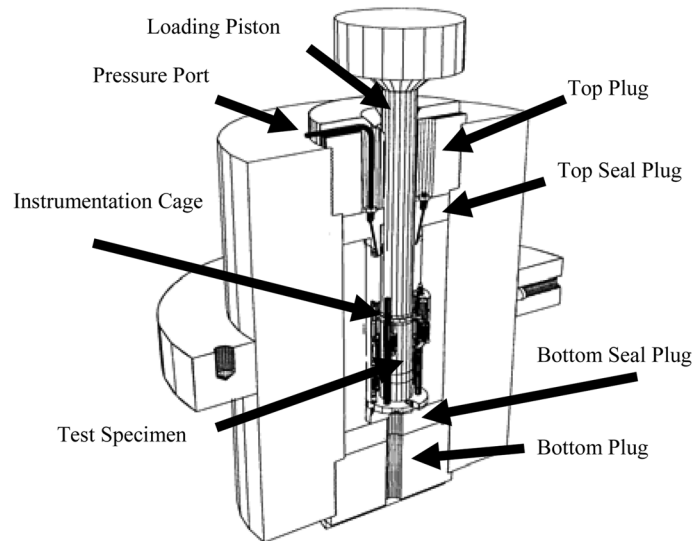


Fig. 1 600-MPa pressure vessel details

The system was programmed for certain rates of load, pressure, and axial displacement to achieve specific stress or strain paths. A pressure transducer mounted in the confining fluid line, measured the confining pressure. A load cell mounted in the base of the specimen pedestal measured the applied axial loads.

The vertical deflection measurement system consisted of two linear variable differential transformers (LVDTs) mounted vertically inside the pressure vessel on an instrumentation stand and positioned 180 deg apart to measure the displacement between the top and base caps, thus providing a measure of the axial deformations of the specimen. In addition, a linear potentiometer was externally mounted to the pressure vessel to measure the displacement of the piston through which axial load was applied, providing a backup to the internal LVDTs in case the deformation exceeded the LVDTs' calibrated range (66.35 mm). Two radial deflection measurement systems were used in this test program. One lateral deformer consisted of an LVDT mounted on a hinged ring; the LVDT measured the expansion or contraction of the ring (Bishop and Henkel, 1962) and was used for smaller ranges of radial deformation when the greatest measurement accuracy (61.27 mm) was required. The second lateral deformer, which was used when the greatest radial deformation range was required, and was therefore less accurate than the LVDT, consisted of two strain-gaged spring-steel arms mounted on a double-hinged ring; the strain-gaged arms deflected as the ring expanded or contracted.

2.2. Test descriptions

The TXC tests were conducted in two phases. During the first phase, the HC phase, the specimen was subjected to an increase in hydrostatic pressure while its height and diameter changes were measured. The second phase of the TXC test, the shear phase, was conducted after the desired confining pressure had been applied during the HC phase. While holding the desired confining pressure constant, the axial load was increased to specimen failure while measurements of the changes in the specimen's height and diameter were made. These tests determined the specimens'

peak strength which is defined as the maximum principal stress difference that a given specimen can support or the principal stress difference at 15 percent axial strain during the shear loading, whichever occurs first.

The UC tests were performed in accordance with ASTM C 39 (ASTM 2009). The UC test is a TXC test in which no confining pressure is applied. The unconfined compressive strength of the material was determined by observing the maximum principal stress difference during the UC test.

Tension shear data were obtained for Cor-Tuf1 and Cor-Tuf2 by performing DP tests on unconfined specimens until the specimen failed.

The UX tests were conducted by applying axial load and confining pressure simultaneously so that, as the cylindrical specimen shortened, its diameter remained unchanged, i.e., zero radial strain boundary conditions were maintained.

The strain-path tests were conducted in two phases. Initially, the specimen was subjected to a UX loading up to a desired level of axial stress. At the end of the UX loading, a constant axial-to-radial-strain ratio of -2.0 was applied; these tests were identified earlier as UX/CV tests. These tests required the software controlling the servo-controls to correct the measured inputs for system compressibility and for the nonlinear calibrations of specific transducers.

3. Analysis of mechanical property test results

During the mechanical property tests, measurements were typically made of the axial and radial deformations of the specimen as confining pressure and/or axial load were applied or removed. These measurements, along with the pretest height and diameter of the specimen, were used to convert the measured test data to true stresses and engineering strains.¹

Axial strain, ε_a , was computed by dividing the measured axial deformation, Δh (change in height), by the original height, h_o , i.e., $\varepsilon_a = \Delta h/h_o$. Similarly, radial strain, ε_r , was computed by dividing the measured radial deformation, Δd (change in diameter), by the original diameter, d_o , i.e., $\varepsilon_r = \Delta d/d_o$. For this report, volumetric strain was assumed to be the sum of the axial strain and twice the radial strain, $\varepsilon_v = \varepsilon_a + 2\varepsilon_r$.

The principal stress difference, q , was calculated by

$$q = (\sigma_a - \sigma_r) = \frac{\text{Axial Load}}{A_o(1 - \varepsilon_r)^2} \quad (1)$$

Where:

q = principal stress difference

σ_a = axial stress

σ_r = radial stress

A_o = original cross-sectional area of the specimen

ε_r = radial strain

The axial stress is related to the confining pressure and the principal stress difference by

$$\sigma_a = q + \sigma_r \quad (2)$$

The mean normal stress, p , is the average of the applied principal stresses. In cylindrical geometry,

¹Compressive stresses and strains are positive in this paper

Table 2 Average composition properties for test specimens

Cor-Tuf Mix	Wet Density Mg/m ³	Water Content, %	Dry Density, Mg/m ³	Air Voids Content, %
1	2.557	2.73	2.490	8.3
2	2.328	3.24	2.256	11.3

$$p = \frac{(\sigma_a + 2\sigma_r)}{3} \tag{3}$$

3.1. Composition properties

Measurements of posttest water content for each test specimen were conducted in accordance with procedures given in ASTM D 2216 (ASTM 2009). Based on the appropriate values of posttest water content, wet density, and specific gravity, the values of dry density and the air voids content of the test specimens were determined. Table 2 lists the average test specimen’s wet density, water content, dry density, and air voids content from each batch of Cor-Tuf.

3.2. Hydrostatic compression test results

Undrained bulk compressibility data were obtained from the HC tests and during the hydrostatic loading phase of the TXC tests. Fig. 2 compares the pressure-volume data from the HC tests conducted on each concrete. The figure legend identifies the test number, then designates whether the test specimen as Cor-Tuf1 or Cor-Tuf2. The initial dry densities of the Cor-Tuf1 HC test specimens were 2.510 and 2.523 Mg/m³, while the initial dry densities of the Cor-Tuf2 HC test specimens were 2.286 and 2.312 Mg/m³. For each material the test specimens with the lower densities (test 3-1 for Cor-Tuf1 and test 3-2 for Cor-Tuf2) were more compressible than the test specimens with the higher densities. The HC compressibility for Cor-Tuf1 and 2 were very similar, with Cor-Tuf2 displaying a slightly greater compressibility. This implies that the slightly increased

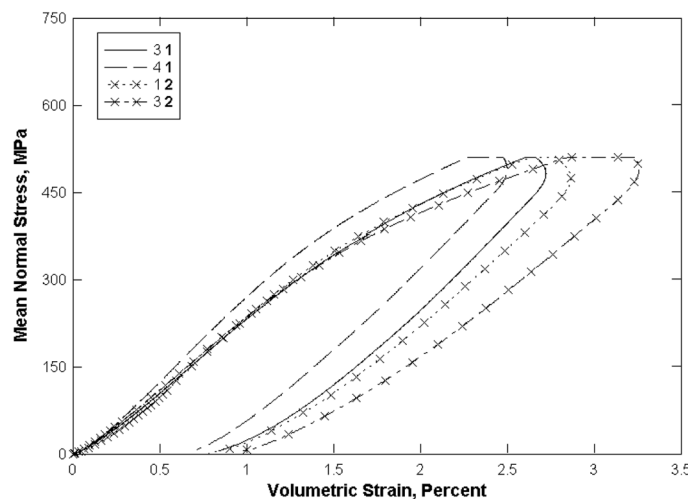


Fig. 2 Pressure-volume responses from HC tests

density and the steel fibers in Cor-Tuf1 reduced its compressibility compared with that of Cor-Tuf2. During the transition from loading to unloading, the pressure was held constant, and the deformations were monitored. When the deformation rate decreased significantly, the pressure was decreased. The volumetric strains of the specimens of both concretes increased during the transition. The increase indicated that the concretes were susceptible to creep. Based on the data from the HC tests, the initial elastic bulk modulus was 25.2 GPa for Cor-Tuf1 and 22.7 GPa for Cor-Tuf2.

3.3. Triaxial compression test results

Compression shear and failure data were obtained from the UC and the unconsolidated-undrained TXC test results. Fig. 3 presents plots of the stress-strain data (principal stress difference versus

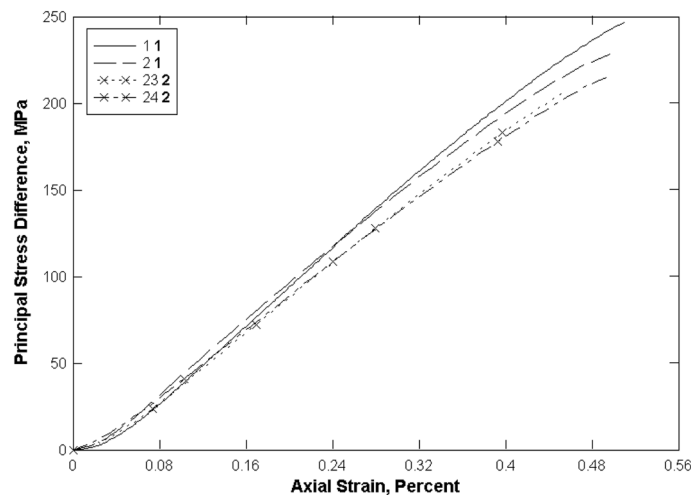


Fig. 3 Stress-strain data from UC tests

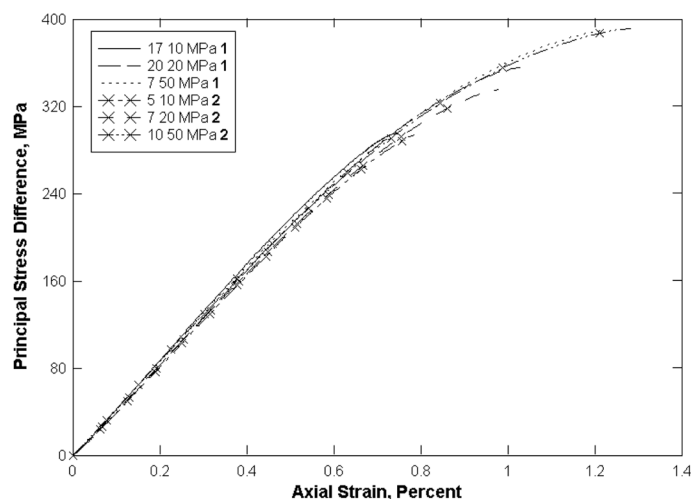


Fig. 4 Stress-strain data from selected TXC tests at constant confining pressures between 10 and 50 MPa from Cor-Tuf1 and Cor-Tuf2

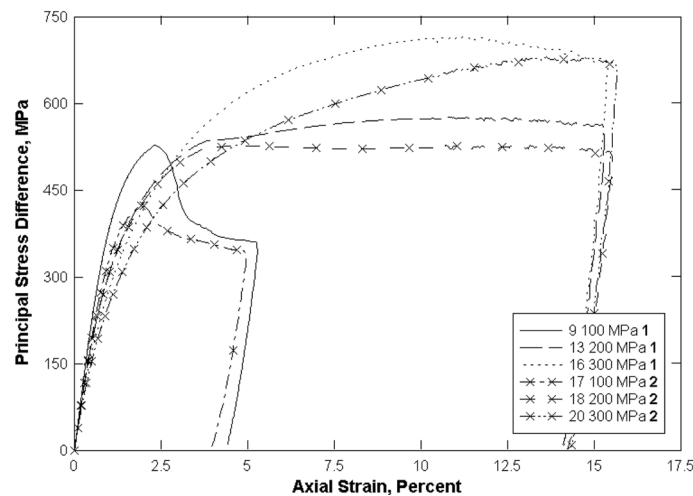


Fig. 5 Stress-strain data from selected TXC tests at confining pressures between 100 and 300 MPa from Cor-Tuf1 and Cor-Tuf2

axial strain) from the UC tests for each concrete. No attempt was made to capture the post-peak (or softening) stress-strain behavior during the UC tests. The UC test results were very sensitive to small changes in the dry density and specimen structure, which caused variations of the initial loadings and peak strengths. The mean unconfined compressive strengths of Cor-Tuf1 and Cor-Tuf2 were 237 and 210 MPa, respectively.

For comparison purposes, Fig. 4 shows stress-strain data from selected TXC tests conducted with constant confining pressures of 10, 20, and 50 MPa, while Fig. 5 shows that data for constant confining pressures of 100, 200, and 300 MPa. The legends for these two figures include the test number, the level of confining pressure, and the number designating the specimen as Cor-Tuf1 or Cor-Tuf2. For plotting purposes, the axial and volumetric strains at the beginning of the shear phase were set to zero, i.e., only the strains during shear are plotted. A general comment should be made concerning the unloading results: the final unloading stress-strain responses at axial strains greater than 11 percent were less reliable than those less than 11 percent because at that point the range of the internal vertical deformeters was exceeded. Beyond that point, an external deformeter with less resolution was used to measure axial displacement.

The peak strengths of the test specimens for Cor-Tuf1 and 2 were very similar for confining pressures between 10 and 50 MPa (Fig. 4). Cor-Tuf1 clearly displayed greater strength than Cor-Tuf2 at confining pressures of 100 MPa and greater (Fig. 5). Cor-Tuf1's increased strength resulted from the higher density of the test specimens and the inclusion of steel fibers.

Fig. 5 illustrates both the brittle and ductile nature of Cor-Tuf1 and Cor-Tuf2. At confining pressures of 100 MPa and below, Cor-Tuf1 and Cor-Tuf2 test specimens behaved in a brittle manner, i.e., the material strain-softened. At confining pressures above 100 MPa, Cor-Tuf1 and Cor-Tuf2 behaved in a ductile manner, i.e., the stress-strain data exhibited strain hardening. Fig. 6 showed that the volumetric strain responses initially displayed compaction followed by dilation during shear for Cor-Tuf1 and 2 for confining pressures of 100 MPa and above.

The failure data and the compression failure surfaces for both concretes developed from the UC and the TXC test results are plotted in Fig. 7 as principal stress difference versus mean normal

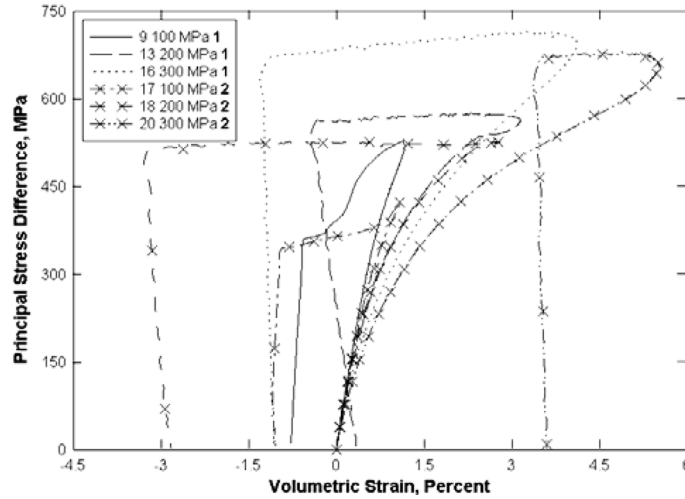


Fig. 6 Stress difference-volumetric strain responses during shear from selected TXC tests at confining pressures between 100 and 300 MPa from Cor-Tuf1 and Cor-Tuf2

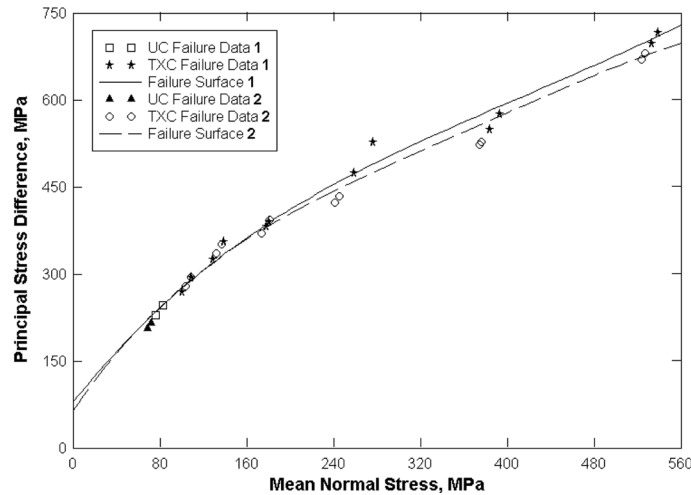


Fig. 7 Failure data from UC and TXC tests and the failure surfaces for both materials

stress. The recommended failure surfaces for Cor-Tuf1 and Cor-Tuf2 were initially the same. However, as the confining pressure increased, Cor-Tuf1's failure surface increased slightly over Cor-Tuf2's. The response data from the 300 MPa TXC tests indicated that neither Cor-Tuf1 nor Cor-Tuf2 had reached void closure. Concrete materials can continue to gain strength with increasing pressure until all of the air porosity in the specimen is crushed out, i.e., when void closure is reached. Void closure can be attained during the shear loading phase of the TXC tests and under hydrostatic loading conditions. The failure surface will have a minimal slope after void closure is achieved.

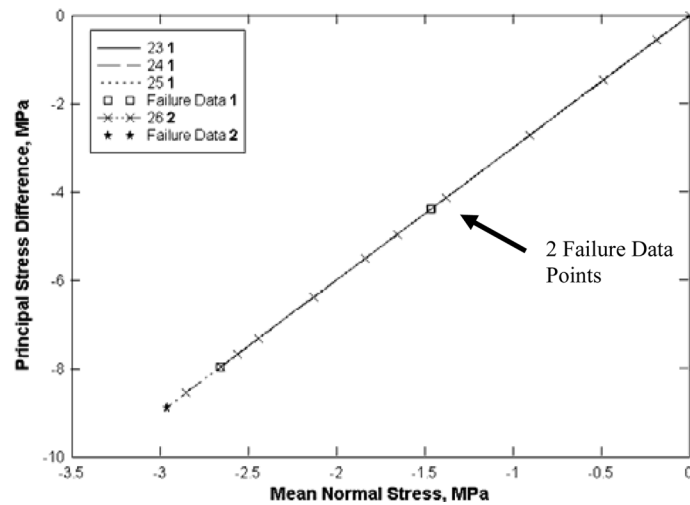


Fig. 8 Stress paths from DP tests and the failure data for Cor-Tuf1 and Cor-Tuf2

3.4. Direct pull test results

Results from the DP tests are plotted in Fig. 8. The average tensile strength from the Cor-Tuf1 DP tests was -5.58 MPa, while the Cor-Tuf2 DP test specimen failed at -8.88 MPa. Only one DP test was completed for Cor-Tuf2 because the high strength epoxy failed in the remaining tests before the test specimens fractured. The average tensile strength of Cor-Tuf1 concrete was 2.4 percent of its average unconfined compressive strength, while the tensile strength of the Cor-Tuf2 concrete was 4.2 percent. According to the American Concrete Institute (ACI) Committee Report 318-02 (ACI 2002), the tensile strength of conventional strength concrete is normally assumed to be about 10 to 15 percent of the unconfined compressive strength. In this case, both Cor-Tuf1 and 2 had less tensile strength than is generally assumed for conventional concrete.

3.5. Uniaxial strain test results

Figs. 9 and 10 compare the UX test results for the two concretes. The stress-strain data are plotted in Fig. 9 and the stress paths with the TXC failure surfaces in Fig. 10. Cor-Tuf2 displayed greater compressibility (greater axial strains) (Fig. 9) than Cor-Tuf1 because the densities and the steel fibers of the Cor-Tuf1 test specimens reduced its compressibility.

From the UX stress-strain loading data in Fig. 9, the initial constrained moduli of Cor-Tuf1 and Cor-Tuf2 were 47.4 and 43.1 GPa, respectively. Initial shear moduli of 16.7 GPa for Cor-Tuf1 and 15.3 GPa for Cor-Tuf2 were calculated based on each concrete's initial constrained modulus and bulk modulus (25.2 GPa for Cor-Tuf1 and 22.7 GPa for Cor-Tuf2), as determined from the HC tests. For each concrete, the constrained and bulk elastic moduli were used to calculate the Young's modulus and Poisson's ratio. The initial Young's moduli were 40.9 GPa for Cor-Tuf1 and 37.5 GPa for Cor-Tuf2. The initial Poisson's ratios were 0.23 for Cor-Tuf1 and 0.22 for Cor-Tuf2.

The UX stress paths (Fig. 10) trended below the recommended TXC failure surfaces even at very low stresses. As the principal stress difference increased, the paths softened slightly. The stress paths softened after the cement bonds started to crush, causing the data to plot below the failure surface.

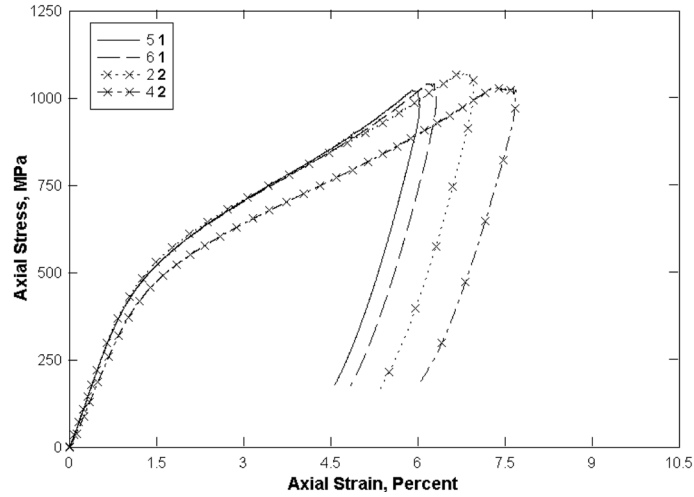


Fig. 9 Stress-strain responses from UX tests

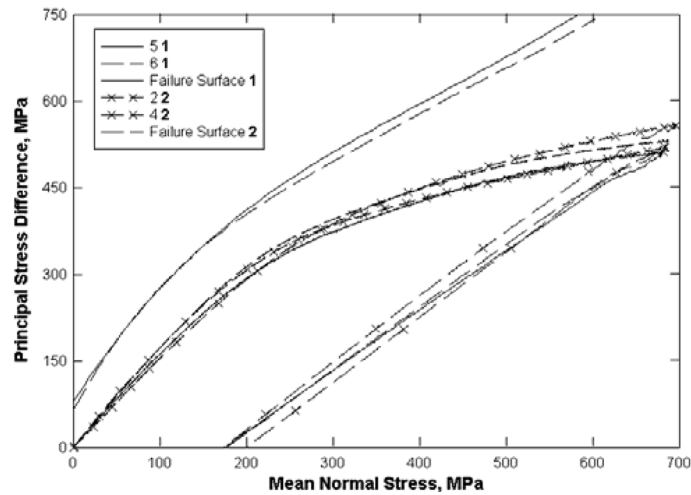


Fig. 10 Stress paths from UX tests and the TXC failure surfaces for Cor-Tuf1 and Cor-Tuf2

The stress paths for both concretes were very similar: both experienced crushing of the cement bonds at a principal stress difference of approximately 300 MPa, and neither displayed full saturation.

3.6. Strain path test results

UX/CV refers to a special strain path test conducted with uniaxial strain loading followed by constant-volumetric-strain loading. Peak axial stresses of approximately 50 and 100 MPa were applied during the UX loading for both materials, although one Cor-Tuf2 test was loaded to 200 MPa. Figs. 11 and 12 compare the results of UX/CV strain-path tests conducted on the two concretes. The pressure-volume data are in Fig. 11, and the stress-paths with the failure surface data are in Fig. 12. Mechanical problems occurred during the CV portion of each test performed on

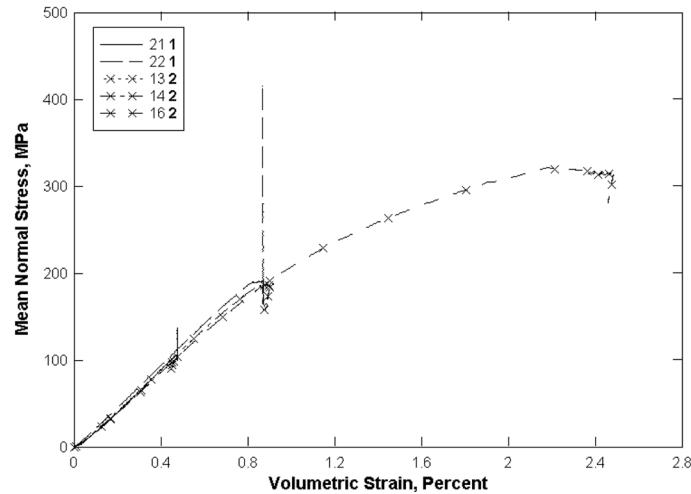


Fig. 11 Pressure-volume data from the UX/CV tests for Cor-Tuf1 and Cor-Tuf2

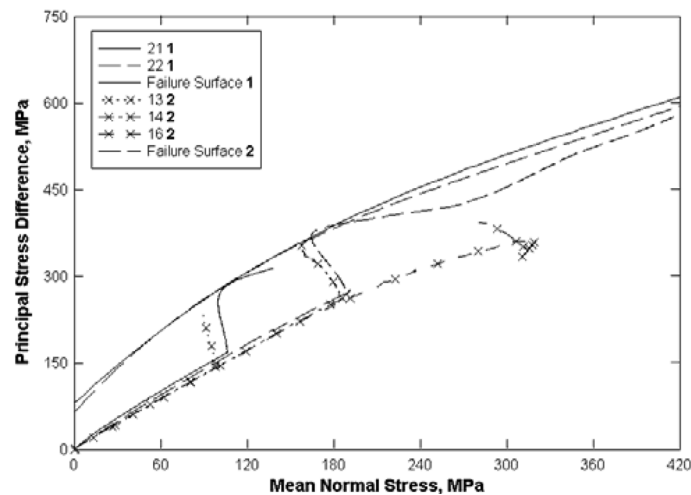


Fig. 12 Stress paths from UX/CV tests and TXC failure surfaces for Cor-Tuf1 and Cor-Tuf2

Cor-Tuf2. The pressure volume data for Cor-Tuf1 (Fig. 11) shows that the specimens were held at a constant volume. Cor-Tuf1 test specimen 22 and Cor-Tuf2 test specimen 14 displayed similar results until the test on specimen 14 was concluded because of a mechanical problem.

4. Conclusions

ERDC personnel conducted a series of laboratory experiments to investigate the constitutive property behavior of ultra-high-performance composite concrete (Cor-Tuf) with and without steel fibers. Twenty-three mechanical property tests were conducted for each batch of Cor-Tuf.

The overall quality of the test data was excellent and repeatable. Cor-Tuf1 and 2 behaved similarly, but Cor-Tuf1 exhibited greater strength with increased confining pressure and less

compressibility than Cor-Tuf2. This is due to the increased density of Cor-Tuf1 and the inclusion of steel fibers. For both materials, creep was observed during the HC tests. Results from each set of TXC tests exhibited a continuous increase in principal stress difference with increasing confining stress. The UC and TXC test results were used to develop the compression failure surfaces and the DP test results established the tensile strengths of the concretes. Comparisons of the unconfined compressive and unconfined tensile strengths showed that both concretes' tensile strengths were less than 10 percent of their unconfined compressive strengths. In addition, the CV loading for Cor-Tuf1 followed closely along the TXC failure surface, validating its failure surface. Overall, the compression tests for the Cor-Tuf concretes were very similar. However, more tensile dominant tests are required to demonstrate the effects of the steel fibers in Cor-Tuf.

Acknowledgments

The tests described and the resulting data presented herein were obtained from research conducted jointly under the Scalable Technology for Adaptive Response and Defeat of Emerging Adaptive Threats Work Packages of the U.S. Army Corps of Engineers, Engineer Research and Development Center, 3909 Halls Ferry Road, Vicksburg, MS 39180-6199. Permission to publish this paper was granted by the Director, Geotechnical and Structures Laboratory.

References

- American Society for Testing and Materials (2009), *Standard practices for preparing rock core as cylindrical test specimens and verifying conformance to dimensional and shape tolerances*, Designation D 4543-04, Philadelphia, PA: American Society for Testing and Materials.
- American Society for Testing and Materials (2009), *Standard test method for compressive strength of cylindrical concrete specimens*, Designation C 39-05, Philadelphia, PA: American Society for Testing and Materials.
- American Society for Testing and Materials (2009), *Standard test method for laboratory determination of water (moisture) content of soil and rock by mass*, Designation D 2216-05, Philadelphia, PA: American Society for Testing and Materials.
- American Concrete Institute (2002), *Building code requirements for structural concrete and commentary*, ACI Committee Report 318, Detroit, MI: American Concrete Institute.
- Bishop, A.W. and D.J. Henkel (1962), *The measurement of soil properties in the triaxial test*, London, Edward Arnold, Ltd.